

Electronic Supplementary Information

Pronounced exciton and coherent phonon dynamics in BiI_3

*Mirko Scholz, Kawon Oum and Thomas Lenzer**

Universität Siegen, Physikalische Chemie, Adolf-Reichwein-Str. 2, 57076 Siegen, Germany,
E-mail: lenzer@chemie.uni-siegen.de

Table of Contents

1. Calculated band structures of BiI_3	2
2. Frequencies of the Raman-active optical phonons for BiI_3	7
3. References.....	8

1. Calculated band structures of BiI₃

DFT calculations for BiI₃ using norm-conserving pseudopotentials within the local density approximation (LDA) Perdew-Zunger functional without spin-orbit coupling (SOC) were carried out using the “Quantum Espresso” package¹ as described in the main manuscript.

The resulting band diagram based on the structure of BiI₃ from literature² is shown in Fig. S1. The maxima in the valence band (VB) and the minima in the conduction band (CB) are indicated as open red and blue circles, respectively. The absolute maximum of the VB is located at *ca.* 0.32 $\overline{\Gamma\text{K}}$, however all the other maxima are only less than 5 meV away. The absolute minimum of the CB is located at the Γ point, yet the minimum at the A point is only about 13 meV away. This calculation therefore predicts an indirect band-gap of 2.25 eV in good agreement with previous DFT calculations by Zhang *et al.*³

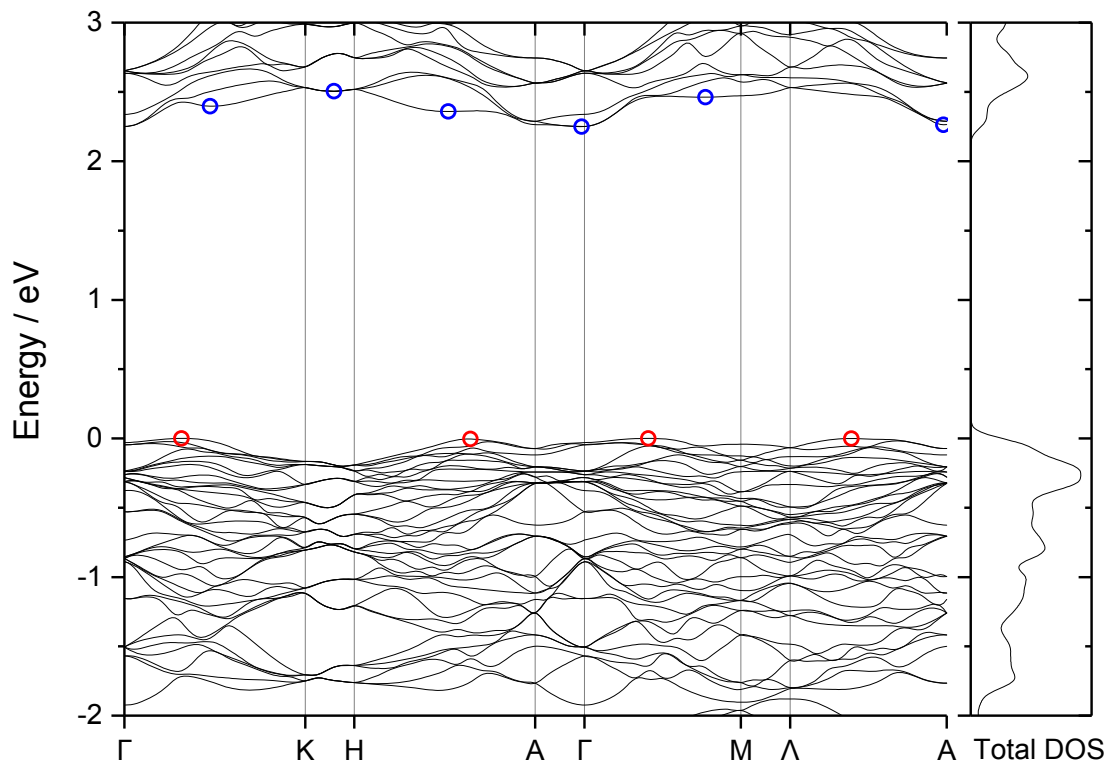


Figure S1. (Left) Calculated band diagram of BiI₃ based on the literature structure of Trotter and Zobel.² High symmetry points of the first Brillouin zone for the primitive hexagonal unit cell are indicated. The open red circles represent energy maxima in the VB whereas open blue circles denote minima in the CB. (Right) Total density of states (DOS).

We also calculated the band diagram based on the relaxed structure of BiI_3 obtained from our DFT calculations. It is shown in Fig. S2. Again the maxima in the valence band (VB) and the minima in the conduction band (CB) are indicated as open red and blue circles, respectively. In this case the absolute maximum of the VB is located at *ca.* $0.19 \overline{\Gamma\text{K}}$, with the other maxima having an energy difference of less than 15 meV. The absolute minimum of the CB is located close to the Γ point, and the minimum near the A point is only about 3 meV higher in energy. This calculation therefore predicts an indirect band-gap of 2.32 eV, close to the value obtained for the experimental structure of BiI_3 .

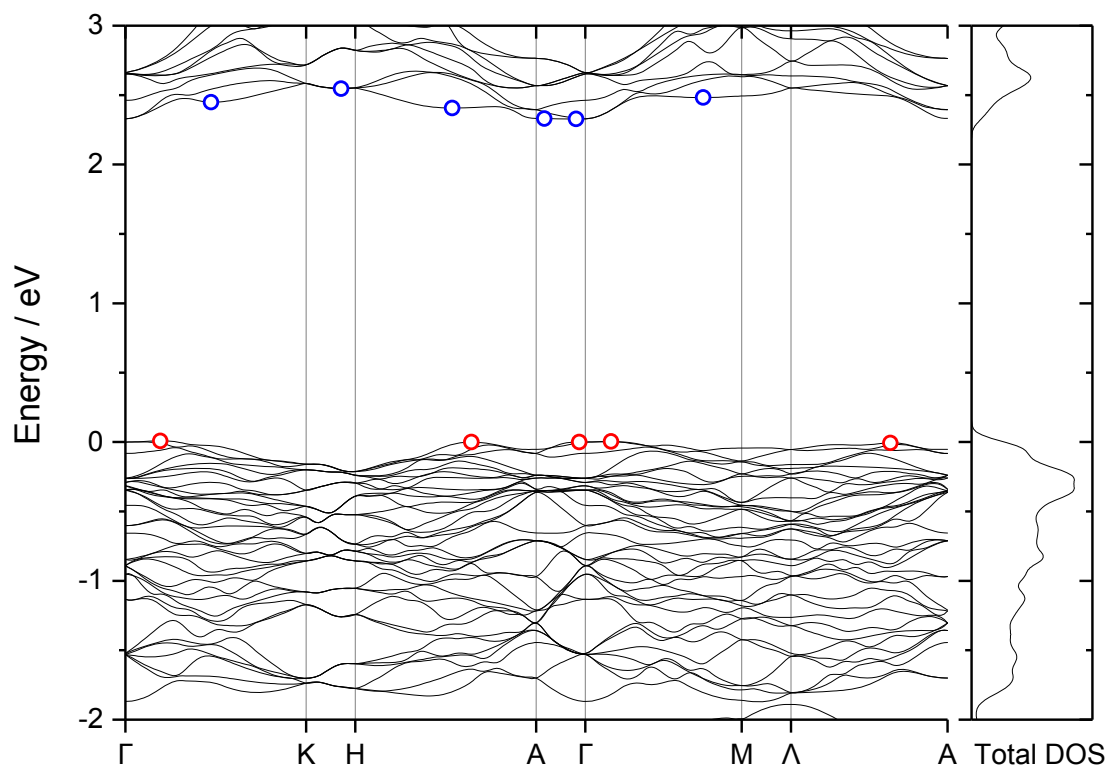


Figure S2. (Left) Calculated band diagram of BiI_3 based on the relaxed structure from our DFT calculations. High symmetry points of the first Brillouin zone for the primitive hexagonal unit cell are indicated. The open red circles represent energy maxima in the VB whereas open blue circles denote minima in the CB. (Right) Total density of states (DOS).

Rhombohedral unit cells were employed for the phonon calculations. The corresponding band diagrams are shown in Fig. S3 and S4, respectively.

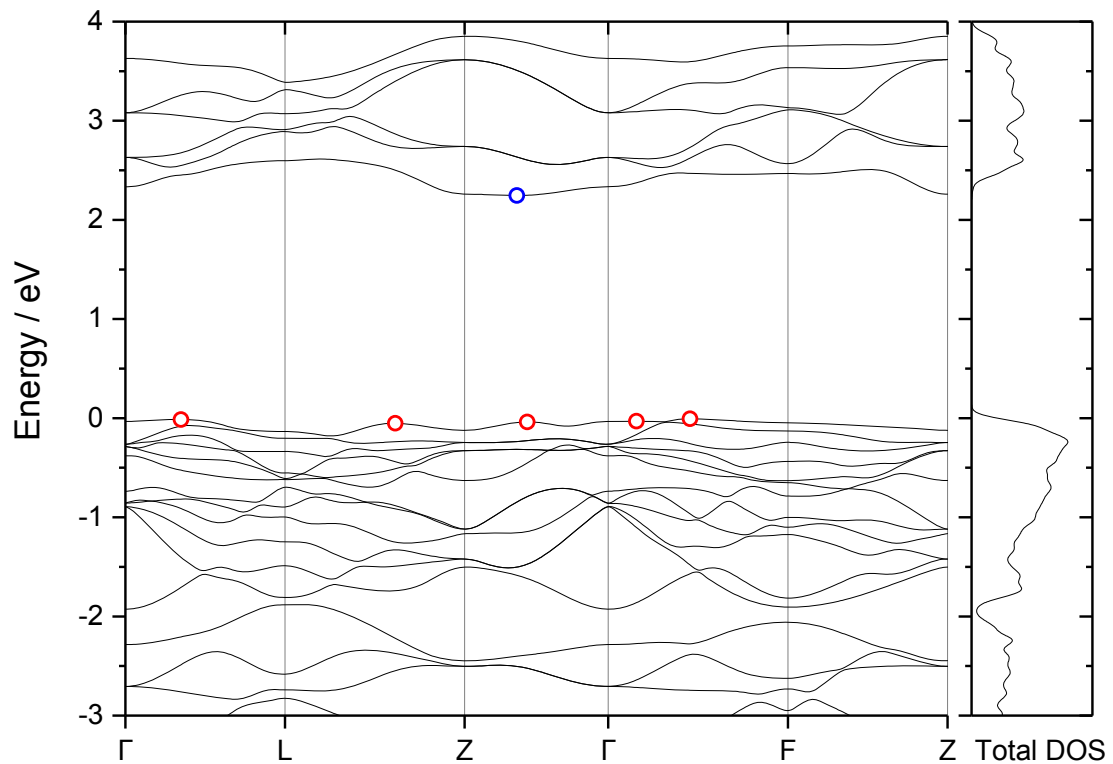


Figure S3. (Left) Calculated band diagram of BiI_3 with relaxed atomic positions from our DFT calculations. High symmetry points of the first Brillouin zone for the rhombohedral unit cell are indicated. The open red circles represent energy maxima in the VB whereas the open blue circle denotes the minimum in the CB. (Right) Total density of states (DOS).

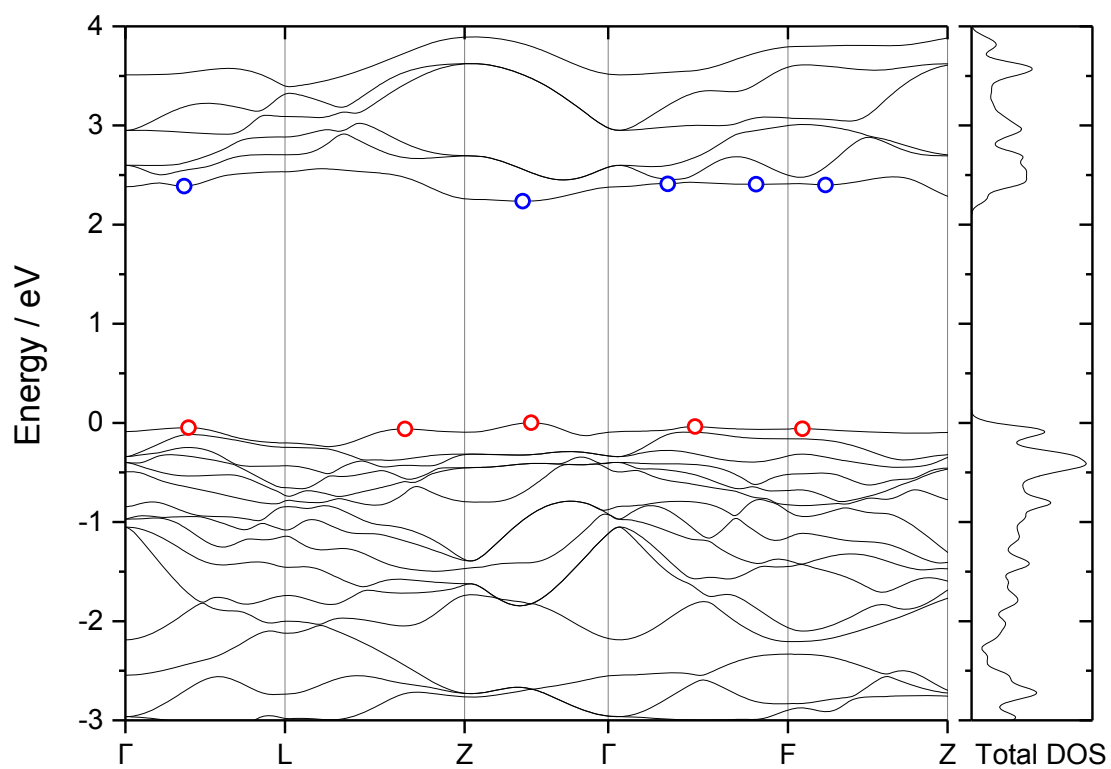


Figure S4. (Left) Calculated band diagram of BiI_3 with relaxed atomic positions and relaxed lattice parameters from our DFT calculations. High symmetry points of the first Brillouin zone for the rhombohedral unit cell are indicated. The open red circles represent energy maxima in the VB whereas open blue circles denote minima in the CB. (Right) Total density of states (DOS).

Structural parameters used for calculating the band diagrams in Fig. S1-S4 are summarised in Table S1, including the available experimental structures.

Table S1 Structural parameters of BiI₃. All bond lengths and distances are in Å.

Structural parameter	Experiment ^a	Hexagonal ^b	Hexagonal ^c	Rhombohedral ^c	Rhombohedral ^d
Bi-I length	3.124	3.121	3.072	3.070	3.072
Bi-I length	3.053	3.045	3.068	3.062	3.047
Bi...Bi distance along c	6.982	6.906	6.938	6.843	6.692
I...I distance along c	3.289	3.336	3.298	3.329	3.104
<i>a</i> = <i>b</i> hexagonal	7.525	7.516	7.516	7.516	7.402
<i>c</i> hexagonal	20.703	20.718	20.718	20.718	20.113
used in Fig.	---	S1	S2	S3	S4

^a Experimental structure from Ruck,⁴ here only given for comparison.

^b DFT calculation based on fixed experimental structure from Trotter and Zobel.²

^c DFT calculation based on structure with relaxed atomic positions.

^d DFT calculation based on structure with relaxed atomic positions and relaxed lattice parameters.

2. Frequencies of the Raman-active optical phonons for BiI₃

A comparison of calculated and experimental Raman frequencies for BiI₃ is shown in Table S2. Our experimental frequencies agree well with the frequencies from DFT calculations (without SOC) by Zhang *et al.* for a single layer of BiI₃ using the PBE functional.³ The comparison with the experimental data of Komatsu *et al.*⁵ shows that the DFT calculations substantially overestimate the frequencies of the E_g modes, whereas for the A_g modes the agreement is better. Especially for the strongest A_g mode, which dominates the spectrum, the deviation is only about 7 cm⁻¹. When using relaxed equilibrium structure lattice parameters all frequencies increase (leading to only 3 cm⁻¹ deviation from experiment for the most intense A_g mode). As shown by Zhang *et al.* introduction of SOC will lower the frequencies of all Raman modes. This reduces the deviations for the E_g modes, but at the same time leads to a larger deviation for the intense A_g mode dominating the spectrum.³

Table S2 Comparison of calculated and experimental frequencies for the Raman-active optical phonons of BiI₃.

Symmetry ^a	$\tilde{\nu}_{\text{rhom}}^b$ (cm ⁻¹)	Intensity ^c (Å ⁴ amu ⁻¹)	$\tilde{\nu}_{\text{rhom,relaxed}}^d$ (cm ⁻¹)	Intensity ^e (Å ⁴ amu ⁻¹)	$\tilde{\nu}_{\text{Zhang}}^f$ (cm ⁻¹)	$\tilde{\nu}_{\text{exp}}^g$ (cm ⁻¹)
E _g	118.5	193	121.6	239	113	95
A _g	106.4	1947	110.4	3612	102	113.3
E _g	94.7	236	96.6	506	89	36.7
A _g	73.5	0.9	79.7	12	61	58.5
E _g	53.8	45	56.1	62	52	33.5
A _g	44.4	190	51.2	275	39	53.5
A _g	35.4	1.4	36.7	2.8	34	22.8
E _g	31.2	3.6	35.5	11.8	28	12.9

^a The E_g modes are doubly degenerate whereas the A_g modes are non-degenerate, therefore 12 modes in total.

^b Calculated phonon frequencies (rhombohedral unit cell, relaxed atomic positions), see Fig. S3 and Table S1.

^c Corresponding intensities for the Raman lines in the second column.

^d Same as for b) but in addition relaxed lattice parameters, see Fig. S4 and Table S1.

^e Corresponding intensities for the Raman lines in the fourth column.

^f Raman frequencies for a single layer of BiI₃ estimated from Fig. 4(a) of Zhang *et al.*³

^g Experimental Raman frequencies of BiI₃ from Komatsu *et al.*⁵

3. References

1. P. Giannozzi, S. Baroni, N. Bonini, M. Calandra, R. Car, C. Cavazzoni, D. Ceresoli, G. L. Chiarotti, M. Cococcioni, I. Dabo, A. Dal Corso, S. de Gironcoli, S. Fabris, G. Fratesi, R. Gebauer, U. Gerstmann, C. Gougoussis, A. Kokalj, M. Lazzeri, L. Martin-Samos, N. Marzari, F. Mauri, R. Mazzarello, S. Paolini, A. Pasquarello, L. Paulatto, C. Sbraccia, S. Scandolo, G. Sclauzero, A. P. Seitsonen, A. Smogunov, P. Umari and R. M. Wentzcovitch, *J. Phys.: Condens. Matter*, 2009, **21**, 395502.
2. J. Trotter and T. Zobel, *Z. Kristallogr., Kristallgeom., Kristallphys., Kristallchem.*, 1966, **123**, 67.
3. W.-B. Zhang, L.-J. Xiang and H.-B. Li, *J. Mater. Chem. A*, 2016, **4**, 19086.
4. M. Ruck, *Z. Kristallogr.*, 1995, **210**, 650.
5. T. Komatsu, T. Karasawa, T. Iida, K. Miyata and Y. Kaifu, *J. Lumin.*, 1981, **24/25**, 679.